Near-wall Modeling of The Nonlinear Turbulence Model for a Rotating Square Duct

Suabsakul Gururatana [1*] and Varangrat Juntasaro [2]

[1] Mechanical Engineering Program, Faculty of Engineering at Si Racha, Kasetsart University, Si Racha, Chonburi 20230, Thailand,
Tel: 0-38354350, Fax: 0-38354849, *Email: g4765080@ku.ac.th
[2] Department of Mechanical Engineering, Faculty of Engineering, Kasetsart University, Bangkhen, Bangkok 10900, Thailand,
Tel: 0-29428555 ext 1829, Email: fengvrj@ku.ac.th

Abstract

The characteristics of flow field in the internal passage of turbine blade cooling are affected by the combined effects of the secondary flows and the rotation of the blade. These secondary flows occur in the near wall regions and have the great effect on the characteristics of the primary flow and the cooling rate. Accurate modeling of the flow in the near wall regions is therefore necessary. This paper aims to analyze the performance of the various near-wall models in predicting the flow field in a rotating square duct when they are implemented in the nonlinear turbulence model. The nonlinear turbulence model used in this work is developed from the most suitable Reynolds-stress expression and the linear base model from the previous works. It is found that the non-equilibrium wall function should be used in the case of the flow through the straight square duct without the rotation effect. The damping function of Craft *et al.* (1996) is more suitable for the case of the rotating square duct as the near-wall modeling for the nonlinear turbulence model.

Keywords: rotating square duct, near-wall modeling, nonlinear eddy viscosity turbulence model, damping function, wall function

1. Introduction

The increase in the efficiency of the gas turbine engine causes the temperature of the gas to rise. However the maximum temperature of the turbine blades is limited by the manufacturing material, the cooling of the blades is necessary for the heat reduction. The important flow characteristics in the turbine blade cooling are the combined effects of the rotating and the secondary flows. A rotating square duct is usually chosen as the test case to represent this kind of flow.

Although the large eddy simulation is more suitable for the flow modeling in the combustor, the Reynolds-averaged Navier-Stokes turbulence model is more suitable for the flow modeling in the turbine. The modeling of the turbulent flows in a rotating square duct is still not satisfactory even for the advanced Reynolds-averaged Navier-Stokes turbulence models like Reynolds stress models, explicit algebraic Reynolds stress models and nonlinear turbulence models (Pettersson Reif and Andersson [1] and Belhoucine *et al.* [2]). The possible errors are the Reynolds-stress expression, the linear base model and the near-wall modeling. The different nonlinear Reynolds-stress expressions were compared by Juntasaro *et al.* [3] using *a priori* method. The Reynolds-stress expression of Craft *et al.* [4] was the most accurate expression in predicting the secondary flows in a straight square duct. The popular linear base turbulence models were evaluated for a rotating square duct by Gururatana *et al.* [5]. It was found that the k-ε turbulence model with the enhanced and the non-equilibrium wall functions were more suitable as the linear base model than the k-ω SST turbulence model. The results also showed that although the explicit algebraic Reynolds stress model was capable of modeling certain aspect of the flow in the rotating square duct, the improvement on the near-wall modeling might prove useful on the suction side and the corner bisector of the duct.

The present work is therefore aimed to analyze the performance of different near-wall models for the chosen nonlinear turbulence model from the previous works. The near-wall models considered in this work are the damping functions, the enhanced wall function and the non-equilibrium wall function.

2. Mathematical Formulation

2.1. Governing Equations

For steady state incompressible rotating turbulent flows, the Reynolds-averaged governing equations can be written in Cartesian tensor notation as

$$\frac{\partial}{\partial x_i}\left(U_i\right) = 0 \qquad (1)$$

$$U_j \frac{\partial}{\partial x_j}\left(U_i\right) = -\frac{1}{\rho}\frac{\partial P}{\partial x_i} + \frac{\partial}{\partial x_j}\left(\nu\frac{\partial U_i}{\partial x_j} - \rho\overline{u_i u_j}\right) - 2e_{ijk}\Omega_j U_k \quad (2)$$

where U_i is mean velocity, u_i is fluctuating velocity, ν is kinematic viscosity, $\overline{u_i u_j}$ is Reynolds-stress tensor, ρ is fluid density, Ω_j is angular velocity and e_{ijk} is permutation tensor

2.2. Near-Wall Modeling for The Nonlinear k-ε Turbulence Models

The nonlinear turbulence models employed in this work are developed from the Reynolds-stress expression of Craft *et al.* [4] with the k-ε turbulence model of Launder and Sharma [6] and the k-ε turbulence model of Launder and Spalding [7] for the low-Reynolds-number and the high-Reynolds-number modeling respectively.

The Reynolds-stress $\left(-\rho\overline{u_i u_j}\right)$ is modeled by the cubic Reynolds-stress expression of Craft *et al.* [4] as follows.

$$a_{ij} \equiv \frac{\overline{u_i u_j} - \frac{2}{3}\delta_{ij}k}{k} \quad (3)$$

$$\begin{aligned} a_{ij} = & -\frac{\nu_t}{k}S_{ij} \\ & + c_1\frac{\nu_t}{\varepsilon}\left(S_{ik}S_{jk} - \frac{1}{3}S_{kl}S_{kl}\delta_{ij}\right) \\ & + c_2\frac{\nu_t}{\varepsilon}\left(\Omega_{ik}S_{jk} + \Omega_{jk}S_{ik}\right) \\ & + c_3\frac{\nu_t}{\varepsilon}\left(\Omega_{ik}\Omega_{jk} - \frac{1}{3}\Omega_{kl}\Omega_{kl}\delta_{ij}\right) \\ & + c_4\frac{\nu_t k}{\varepsilon^2}\left(S_{ki}\Omega_{lj} + S_{kj}\Omega_{li}\right)S_{kl} \\ & + c_5\frac{\nu_t k}{\varepsilon^2}\left(\Omega_{il}\Omega_{lm}S_{mj} + S_{il}\Omega_{lm}\Omega_{mj} - \frac{2}{3}S_{lm}\Omega_{mn}\Omega_{nl}\delta_{ij}\right) \\ & + c_6\frac{\nu_t k}{\varepsilon^2}S_{ij}S_{kl}S_{kl} \\ & + c_7\frac{\nu_t k}{\varepsilon^2}S_{ij}\Omega_{kl}\Omega_{kl} \end{aligned} \quad (4)$$

Where

$$\tilde{S} \equiv \frac{k}{\varepsilon}\left(1/2S_{ij}S_{ij}\right)^{\frac{1}{2}} \quad (5)$$

$$\tilde{\Omega} \equiv \frac{k}{\varepsilon}\left(1/2\Omega_{ij}\Omega_{ij}\right)^{\frac{1}{2}} \quad (6)$$

$$S_{ij} = \left(\frac{\partial U_i}{\partial x_j} + \frac{\partial U_j}{\partial x_i}\right) \quad (7)$$

$$\Omega_{ij} = \left(\frac{\partial U_i}{\partial x_j} + \frac{\partial U_j}{\partial x_i}\right) - \varepsilon_{ijk}\Omega_k \quad (8)$$

The eddy viscosity can be written as

$$\nu_t = c_\mu f_\mu \frac{k^2}{\varepsilon} \quad (9)$$

where the expression for the c_μ and f_μ can be written as

$$C_\mu = \frac{0.3}{1+0.35\left(max\left(\tilde{S},\tilde{\Omega}\right)\right)^{1.5}} \times\left(1 - exp\left(\frac{-0.36}{exp\left(-0.75\,max\left(\tilde{S},\tilde{\Omega}\right)\right)}\right)\right) \quad (10)$$

$$f_\mu = 1 - exp\left[-\left(Re_t/90\right)^{\frac{1}{2}} - \left(Re_t/400\right)^2\right] \quad (11)$$

where $Re_t = \frac{k^2}{\nu\varepsilon}$, Re_t is turbulent Reynolds number, a_{ij} is Reynolds-stress anisotropy tensor, k is turbulent kinetic energy, δ_{ij} is Kronecker delta, ν_t is eddy viscosity, S_{ij} is mean strain rate tensor, ε is dissipation rate of k, Ω_{ij} is mean vorticity tensor, ε_{ijk} is alternating tensor and the coefficients c_1 to c_7 are given by $c_1 = -0.1,\quad c_2 = 0.1,\quad c_3 = 0.26,\quad c_4 = -10C_\mu^2,\quad c_5 = 0,\quad c_6 = -5C_\mu^2$ and $c_7 = 5C_\mu^2$.

Additionally, Juntasaro *et al.* [3] has found by using *a priori* method that the damping function of Gibson and Dafa'Alla [8] can predict the mean spanwise velocity profile closer to the DNS data than the original damping function of Craft *et al.* [4] especially in the near wall region. The damping function of Gibson and Dafa'Alla [8] can be written as

$$f_\mu = exp\left[-6/\left(1+\frac{Re_t}{50}\right)^2\right] \times\left[1+3\,exp\left(-\frac{Re_t}{10}\right)\right] \quad (12)$$

According to Gururatana *et al.* [5], the results showed that the linear k-ε turbulence model with the enhanced wall function of Kader [9] (hereafter referred to as EWF) and the linear k-ε turbulence model with the non-equilibrium wall function of Kim and Choudhury [10] (hereafter referred to as NEWF) are the suitable linear base models for a rotating square duct.

This work therefore compares the enhanced wall function, the non-equilibrium wall function, the damping function of Craft *et al.* [4] and the damping function of Gibson and Dafa'Alla [8] to find the most appropriate near-wall model for the cubic Reynolds-stress expression of Craft *et al.* [4].

3. Boundary Conditions

The first test case is the fully-developed turbulent channel flow of Kim *et al.* [11] at Reynolds number of 180 based on the friction velocity and the channel half width as shown in Figure 3.

The second test case is the fully-developed turbulent flow through a straight square duct (Figure 4). The results are compared with the DNS data of Gavrilakis [12] at Reynolds number of 4410 based on the bulk velocity and the hydraulic diameter. Figure 4 shows the duct with the reference axis. The x axis designates the streamwise direction. The cross-stream direction is parallel to the y axis and the spanwise direction is parallel to the z axis. The computation domain is one quadrant of the square duct with the symmetry condition at the centre.

The third test case is the fully-developed turbulent flow through a rotating square duct (Figure 5). The results are compared with the DNS data of Martensson *et al.* [13] at Reynolds number of 4400 based on the bulk velocity and the hydraulic diameter with the rotating numbers(Ro) of 0.055 and 0.11, where $Ro = U_o / \Omega L$, U_o is bulk velocity, Ω is angular velocity and L is width of the duct. Figure 5 shows the duct with the reference axis. The x axis designates the streamwise direction. The cross-stream direction is parallel to the y axis and the spanwise direction is parallel to the z axis.

4. Numerical Methods

In this work, the governing equations are discretized by using the finite volume method with the second order upwind scheme. The coupling of the pressure and the velocity is achieved through the SIMPLE algorithm. The convergence criterion is 10^{-4} for all cases. The first point of y^+ is approximately within the limit of the models. The grid-independent study is made for all models as detailed as the maximum limit of the available computing performance.

5. Results and Discussion

5.1. Fully-Developed Turbulent Channel Flow

Figure 6 shows the prediction of the mean streamwise velocity profile compared with the DNS data. The trends of the nonlinear models are generally similar to the DNS data. At the near wall region (y^+=1), the enhanced wall function with the cubic Reynolds-stress expression of Craft *et al.* [4] is better than the other models.

5.2. Fully-Developed Turbulent Flow Through a Straight Square Duct

This section shows the results obtained for a turbulent flow in a square duct. The comparison amongst the models is made with the DNS data of Gavrilakis (1992). The profiles of the mean streamwise velocity are shown in Figure 7 and Figure 8 for y/h = 0.16 and y/h = 0.5, respectively. These figures show the comparison amongst the DNS data, the damping function of Craft *et al*. [4], the damping function of Gibson and Dafa'Alla [8], the enhanced wall function and the non-equilibrium wall function. At y/h = 0.16 (Figure 7), the DNS data show the strong distortion induced by the secondary flows. The damping functions and wall functions are incapable of predicting the distortion on the mean streamwise velocity profile. At the near wall region, the damping function of Craft *et al.* [4] shows the better result than the other models. At y/h = 0.5 (Figure 8), the trend of the mean streamwise velocity profile using the damping functions and the wall functions generally agrees with the DNS data with the overprediction of the velocity.

The comparison between the DNS data and the various models for the cross-stream velocity profile is presented in Figure 9 and Figure 10 for y/h = 0.16 and y/h = 0.5, respectively. At y/h = 0.16 (Figure 9), the DNS data show the strong mean cross-stream velocity profile. The damping functions and the wall functions can not predict this strong velocity profile. At y/h = 0.5 (Figure 10), the damping functions and the wall functions can predict the trend of the velocity profile. At the near wall region, the non-equilibrium wall function can predict the result closer to the DNS data than the other models.

The comparison between the DNS data and the various models for the spanwise velocity is presented in Figure 11 and Figure 12 for y/h = 0.16 and y/h = 0.5, respectively. At y/h = 0.16 (Figure 11), the DNS data show the strong spanwise velocity profile at the near wall region. The damping functions and the wall functions can not predict the strong velocity profile similarly to the cross-stream velocity profile. At the core of the duct (z/h = 1.0), the non-equilibrium wall function can reasonably predict the velocity profile. At y/h = 0.5 (Figure 12), the strong velocity profile occurs at the near wall region similarly to that at y/h = 0.16. The trend of the damping functions and the wall functions is similar to the DNS data. The damping function of Craft *et al.* [4] shows the little better prediction than the other models.

This section shows the performance of the near-wall models in predicting the primary and the secondary flows in a straight square duct. The overall results show that the performance of the non-equilibrium wall function with the cubic Reynolds-stress expression of Craft *et al.* [4] is suitable for the prediction of the primary and the secondary flows in a straight square duct.

5.3. Fully-Developed Turbulent Flow Through a Rotating Square Duct

The comparison between the DNS data and the various models for the streamwise velocity is presented in Figure 13 and Figure 14 for z/h = 0.5 at rotating numbers of 0.055 and 0.11, respectively. Figure 13 and Figure 14 illustrate the strong distortion of the mean streamwise velocity profile. This distortion of the mean streamwise velocity comes from the effect of rotating. At *Ro* = 0.055 (Figure 13), the non-equilibrium wall function can not predict the effect of the distortion. The damping function of Craft *et al.* [4] can predict the effect of the distortion better than the damping function of Gibson and Dafa'Alla [8] and the enhanced wall function. At *Ro* = 0.11 (Figure 14), the damping functions and the wall functions can not predict the effect of distortion.

Figure 15 and Figure 16 show the comparison between the DNS data and the various models for the streamwise velocity at y/h = 0.5 and rotating numbers of 0.055 and 0.11, respectively. At the core region of the duct for both rotating numbers, the spanwise velocity profile of the DNS data is flat. At the near wall region, there is a peak in the velocity profile on both sides of the wall. At *Ro* = 0.055 (Figure 15), the damping function of Craft *et al.* [4] can predict the flatness of the velocity profile better than the damping function of Gibson and Dafa'Alla [8] and the enhanced wall function. The non-equilibrium wall function can not predict this effect. At *Ro* = 0.11 (Figure 16), the damping functions and the wall functions can not predict the flatness of the velocity profile.

This section shows the performance of the near-wall models in predicting the characteristic of the flow field in a rotating straight square duct. The overall results show that the performance of the damping function of Craft *et al.* [4] is the most suitable for the prediction of the flow field characteristic in the rotating straight square duct.

6. Conclusion

The Reynolds-stress expression of Craft *et al.* [4] with the damping function of Craft *et al.* [4], the damping function of Gibson and Dafa'Alla [8], the enhanced wall function and the non-equilibrium wall function are compared with the DNS data for fully-developed turbulent channel flow, fully-developed turbulent flow through a straight square duct and fully-developed turbulent flow through a rotating square duct. In the case of the square duct, the overall result shows that the performance of the non-equilibrium wall function with the cubic Reynolds-stress expression of Craft *et al.* [4] is the most suitable near-wall model to predict the flow field characteristic in the straight square duct. However, the damping function of Craft *et al.* [4] is more suitable when the rotating effect is dominated as in the case of the rotating square duct.

Acknowledgments

This research work is partly supported by the Thai National Grid Project and the SUN Microsystems. The financial supports from the Kasetsart University Research and Development Institute (KURDI), the Commission on Higher Education and the Thailand Research Fund (TRF) for the Senior Scholar Professor Pramote Dechaumphai and the Scholar Associate Professor Varangrat Juntasaro are also acknowledged.

References

[1] Pettersson Reif, B.A. and Andersson, H.I., 2003. Turbulent Flow in a Rotating Duct: A Modeling Study. Journal of Turbulence, Vol. 4, pp. 1-17.

[2] Belhoucine, L., Deville, M., Elazehari, A.R. and Bensalah, M.O., 2004. Explicit Algebraic Reynolds Stress Model of Incompressible Turbulent Flow in Rotating Square Duct. Computers & Fluids, Vol. 33, pp. 179-199.

[3] Juntasaro, V., Gururatana, S., Buranarote, J. and Juntasaro, E., 2005. A New Reynolds-Stress Expression Based on DNS Data in Nonlinear Eddy-Viscosity Turbulence Model for Complex Flows. The Fourth International Symposium on Turbulence and Shear Flow Phenomena (TSFP 4). Virginia, U.S.A.

[4] Craft , T.J., Launder, B.E. and Suga, K., 1996. Development and Application of a Cubic Eddy-Viscosity Model of Turbulence. International Journal of Heat and Fluid Flow, Vol.17, pp. 108-115.

[5] Gururatana, S., Juttijudata, V., Juntasaro E. and Juntasaro, V., 2006. Prediction 3D Turbulence Induced Secondary Flows in Rotating Square Duct. Whither Turbulence Prediction and Control. Seoul national university, Seoul, Korea.

[6] Launder, B.E., Sharma, B., 1974. Application of The Energy Dissipation Model of Turbulence to The Calculation of Flow Near a Spinning Disc. Lett. Heat and Mass Transfer, Vol. 1, pp. 131-138.

[7] Launder, B.E. and Spalding, D.B., 1972. Lecture in Mathematical Models of Turbulence. Academic Press, London, England.

[8] Gibson, M.M. and Dafa'Alla, A.A., 1994. The $q-\zeta$ Model for Turbulent Wall Flow. Proc. 47th Annual Meeting of the Fluid Dynamics Division, American Physical Society, Atlanta, GA, U.S.A.

[9] Kader, B., 1993. Temperature and Concentration Profiles in Fully Turbulent Boundary Layers, International Journal of Heat and Mass Transfer, Vol. 24, pp. 1541-1544.

[10] Kim, S. E., and Choudhury, D., 1995. A Near-Wall Treatment Using Wall Functions Sensitized to Pressure Gradient. ASME FED 217, ASME.

[11] Kim, J., Moin, P. and Moser, R., 1987. Turbulent Statistics in Fully Developed Channel Flow at Low Reynolds Number. Journal of Fluid Mechanic, Vol. 177, pp. 133-166.

[12] Gavrilakis, E., 1992. Numerical Simulation of Low-Reynolds Number Turbulence Flow Through a Straight Square Duct. Journal of Fluid Mechanic, Vol. 244, pp. 101-129.

[13] Martensson, G.E., Brethouwer, G. and Johansson, A.V., 2005. Direct Numerical Simulation of Rotating Turbulent Duct Flow. The Fourth International Symposium on Turbulence and Shear Flow Phenomena (TSFP 4). Virginia, U.S.A.

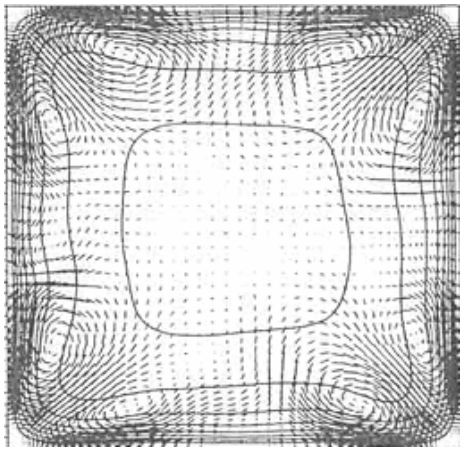

Figure 1. Secondary flows in a straight square duct. (Gavrilakis [12])

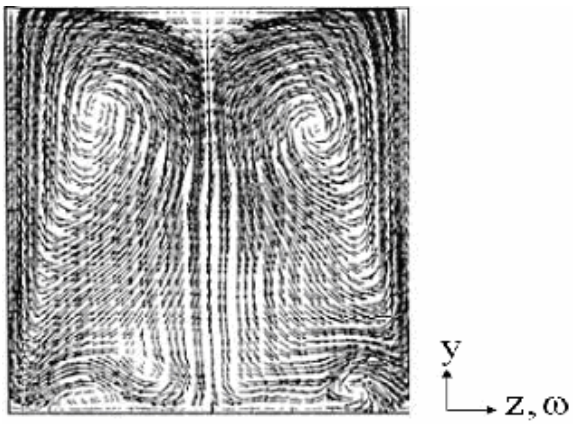

Figure 2. Secondary flows in a rotating straight square duct. (Belhoucine *et al.* [2])

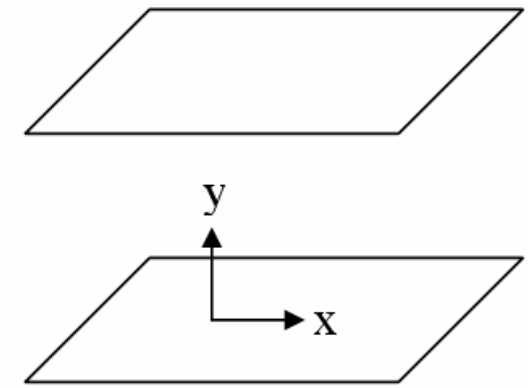

Figure 3. Geometry and coordinate system of the fully-developed turbulent channel flow.

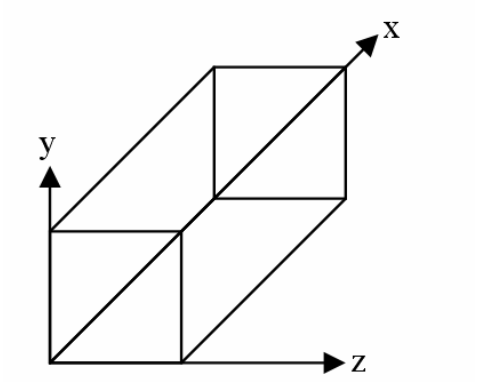

Figure 4. Geometry and coordinate system of the fully-developed turbulent flow through a straight square duct.

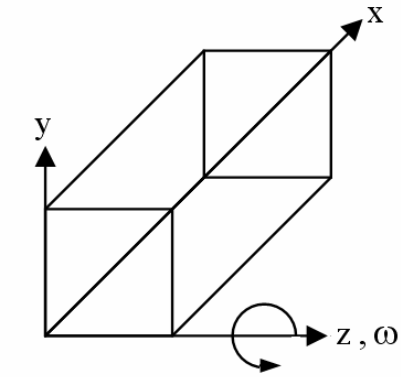

Figure 5. Geometry and coordinate system of the fully-developed turbulent flow through a rotating square duct.

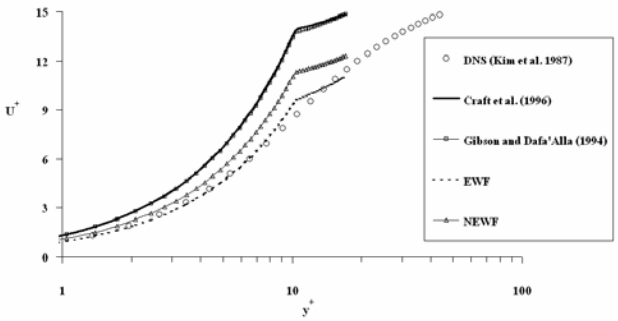

Figure 6. The dimensionless mean streamwise velocity profiles for the fully-developed turbulent channel flow.

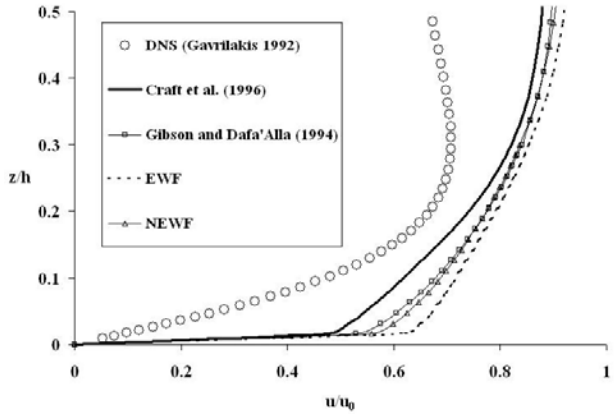

Figure 7. The dimensionless mean streamwise velocity profiles at y/h = 0.16 for the fully-developed turbulent flow through a straight square duct.

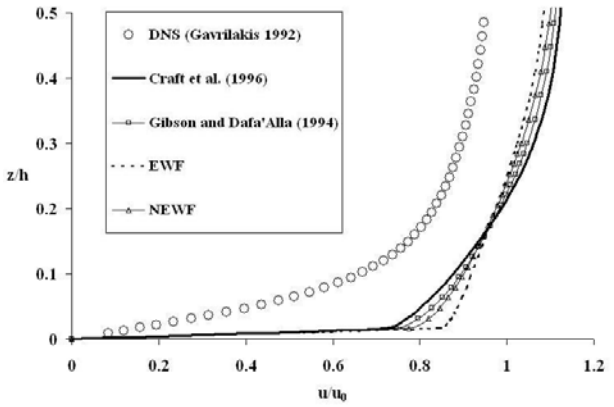

Figure 8. The dimensionless mean streamwise velocity profiles at y/h = 0.5 for the fully-developed turbulent flow through a straight square duct.

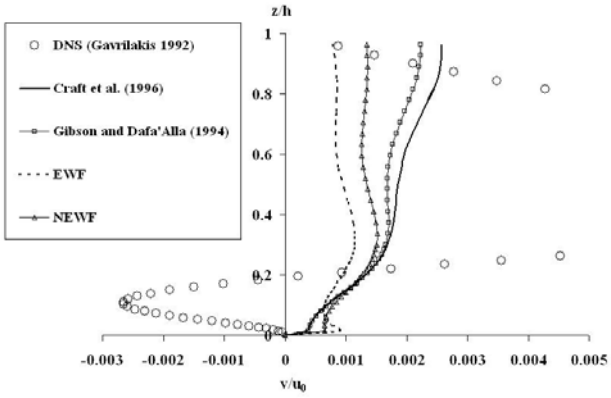

Figure 9. The dimensionless mean cross-stream velocity profiles at y/h = 0.16 for the fully-developed turbulent flow through a straight square duct.

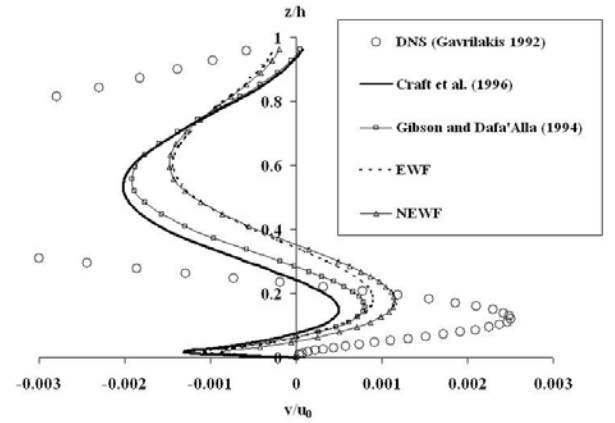

Figure 10. The dimensionless mean cross-stream velocity profiles at y/h = 0.5 for the fully-developed turbulent flow through a straight square duct.

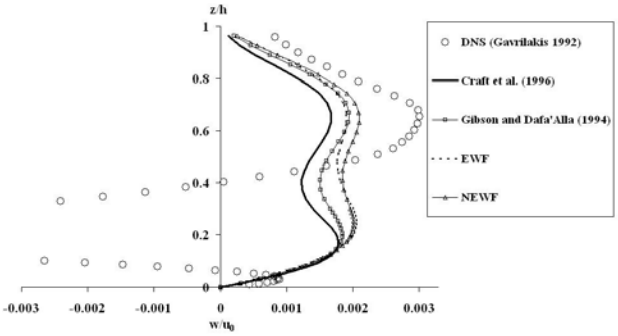

Figure 11. The dimensionless mean spanwise velocity profiles at y/h = 0.16 for the fully-developed turbulent flow through a straight square duct.

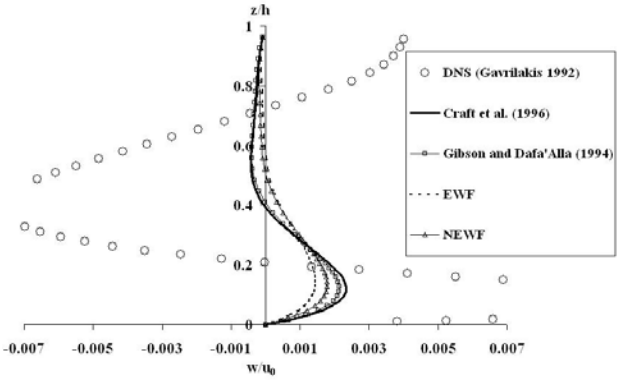

Figure 12. The dimensionless mean spanwise velocity profiles at y/h = 0.5 for the fully-developed turbulent flow through a straight square duct.

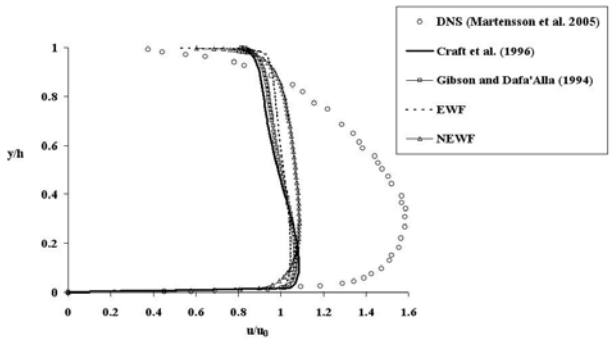

Figure 13. The dimensionless mean streamwise velocity profiles at z/h = 0.5 and *Ro* = 0.055 for the fully-developed turbulent flow through a rotating square duct.

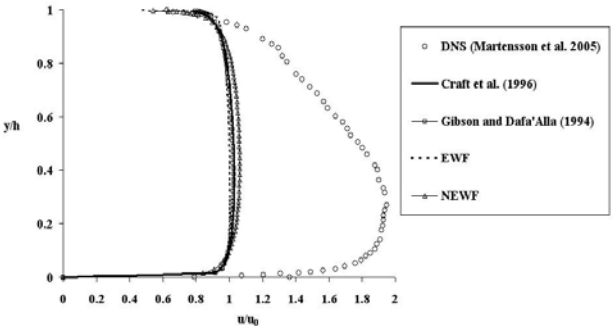

Figure 14. The dimensionless mean streamwise velocity profiles at z/h = 0.5 and *Ro* = 0.11 for the fully-developed turbulent flow through a rotating square duct.

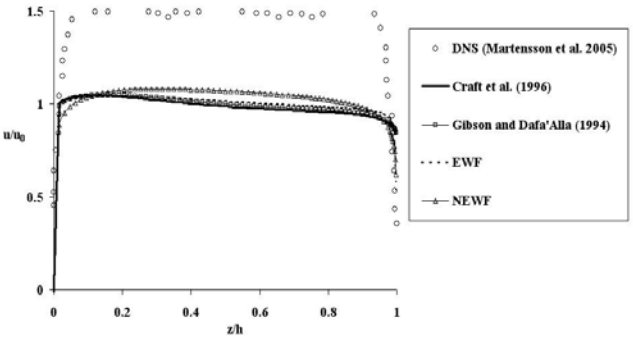

Figure 15. The dimensionless mean streamwise velocity profiles at y/h = 0.5 and *Ro* = 0.055 for the fully-developed turbulent flow through a rotating square duct.

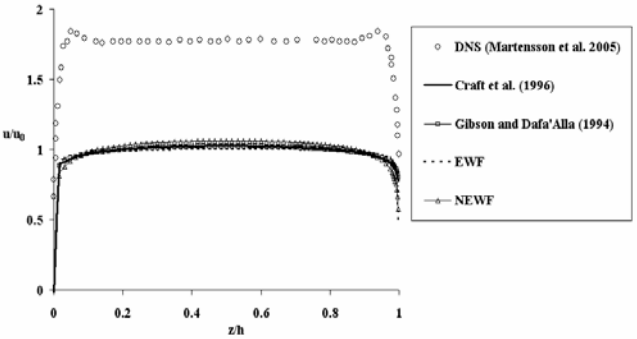

Figure 16. The dimensionless mean streamwise velocity profiles at y/h = 0.5 and *Ro* = 0.11 for the fully-developed turbulent flow through a rotating square duct.